Available online at www.sciencedirect.com
ScienceDirect
Journal of Nuclear Materials 377 (2008) 298–306
journal of nuclear materials
www.elsevier.com/locate/jnucmat

Irradiation damage to the beam window in the 800MWth accelerator-driven system

Kenji Nishihara *, Kenji Kikuchi

Nuclear Transmutation Technology Group, Basic Nuclear Technology and Reactor Engineering Unit, Nuclear Science and Engineering Directorate, Japan Atomic Energy Agency, Tokai-mura, Naka-gun, Ibaraki-ken 319-1195, Japan

Abstract

Irradiation damage to the beam window in the concept of 800MWth accelerator-driven system is evaluated. Heat produced in the window is also evaluated. Transport of proton and neutron up to 3.0 GeV is calculated by both PHITS that is the Monte Carlo code for particles and heavy ions and TWODANT that is two-dimensional deterministic transport code. The beam window is irradiated at the center of the accelerator-driven system with 20 MW proton beam power and neutron from the core during 300 full power days. Heat, displacement per atom, production rate of hydrogen and helium isotopes, and neutron and proton fields are estimated, assuming the Gaussian and flat beam profiles.
© 2008 Elsevier B.V. All rights reserved.

1. Introduction

An accelerator-driven system (ADS) is proposed to transmute minor actinide (MA) to ease the burden of high level waste disposal. In particular, one of the most key components in the ADS is a beam window. In a design of Japan Atomic Energy Agency (JAEA) [1] the beam window positions above the lead–bismuth eutectic (LBE) target and is cooled by LBE. The beam window is not only subjected to the hot LBE under high LBE pressure and thermal stress but also damaged by high energy protons and neutrons. In the ADS design, proton beam energy and criticality mainly affect the amount of irradiation damage. The damage, that is displacement per atom (DPA) and production of hydrogen and helium, is evaluated in the present report. Heat generated in the window is also evaluated.

For the evaluation, flux of the proton and neutron is calculated by the PHITS [2] (particle and heavy ion transport code system) and TWODANT [3] (two-dimensional diffusion-accelerated neutral-particle transport code system). Displacement by proton and neutron above 150 MeV and production of hydrogen and helium by high energy particle above 20 MeV are also calculated by PHITS. DPA cross section below 150 MeV is calculated by processing LA-150 by NJOY code [4]. Cross sections in a library of DCHAIN-SP [5] are available for production of hydrogen and helium by neutron below 20 MeV.

The damage to the window is calculated for the ADS with several parameters those are proton beam energy, criticality, window material and beam shape. The approximate expressions of the damage are induced as functions of these ADS parameters. Then, result of the survey for effects of the ADS parameters to the damage are discussed.

2. ADS design parameter

The proposed ADS is 800MWth, LBE-cooled, tank-type reactor as shown in Fig. 1 and Table 1. The spallation target is also LBE. The core is composed by MA nitride fuel with zirconium nitride to dilute the fuel. The plutonium is added to the fuel only at the initial loading of the first cycle to reduce the burn-up swing of reactivity (Fig. 2). Although in the reference core design [1], two-zone fuel loading is adopted to decrease the power peaking, a

* Corresponding author. Tel.: +81 29 282 5059; fax: +81 29 282 5671.
E-mail address: nishihara.kenji@jaea.go.jp (K. Nishihara).

0022-3115/$ - see front matter © 2008 Elsevier B.V. All rights reserved.
doi:10.1016/j.jnucmat.2008.02.045

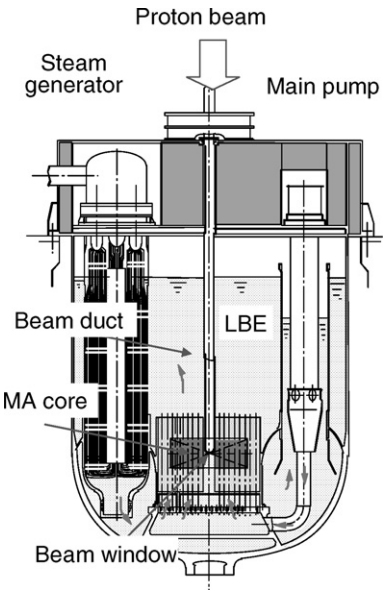

Fig. 1. Conceptual design of 800MWth ADS plant.

Table 1
ADS plant specification

Power (MWth)	800
Cycle length (FPDs)	600
Number of batch	1
k (min/max)	0.94/0.97
Active core diameter (mm)	2343
Active core height (mm)	1000
Coolant temperature (in/out)	300/407
Maximum coolant flow rate (m/s)	2.0
Beam duct diameter (mm)	450
Thickness of beam window (mm)	2
Accelerator type	Proton linac
Beam energy (GeV)	1.5
Beam current (min/max) (mA)	9.6/21

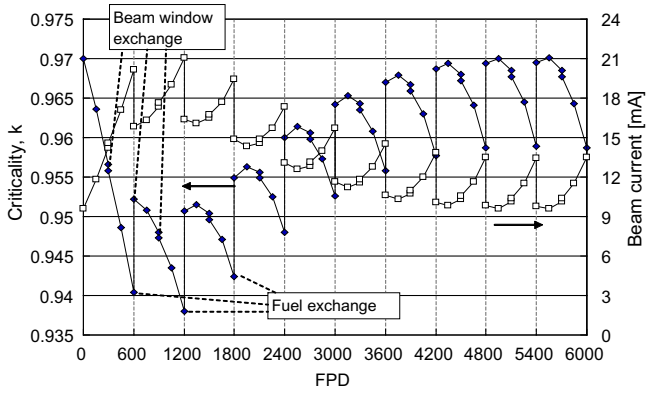

Fig. 2. Swing of criticality and beam current.

single-zone fuel loading is adopted in the present study to simplify the ADS design. The burn-up swing of criticality (k) and proton beam current are almost similar between the single and two-zone fuel loading. However, the low energy neutron from the single-zone MA core to the window material is larger than that from two-zone fuel because the power near the window is higher in the single-zone core than two-zone core.

All the fuel in the core is simultaneously to be unloaded at every 600 full power days (FPDs), while the beam window is to be exchanged at every 300 FPDs by an operation scenario.

The proton beam energy is set at 1.5 GeV. The beam current changes between 9.6 and 21 mA according to criticality swing as shown in Fig. 2. The window is the most irradiated during 900–1200 FPDs.

The detail design around the window is described in Ref. [6]. The target region is separated by a wall from the MA fuel to keep the cooling performance of the MA fuel. The flow control nozzle is positioned under the target to cool the window effectively. When 20 mA proton beam with energy of 1.5 GeV is induced, the heat density at the center was 700 W/cm^3 according to Ref. [6]. The window was designed under the most severe condition, 700 W/cm^3, because the proton beam current is the strongest at 20 mA. The outer surface temperature at center of the window was 450 °C. The maximum temperature was found at the peripheral region, and its value was 490 °C. The maximum velocity of LBE along the window was 1.8 m/s.

3. Calculation method

Flux and cross section of proton and neutron are necessary to evaluate the damage to the window. For the flux of proton and high enrgy neutron above 10 MeV, PHITS is used. PHITS is also available for neutron below 10 MeV using MCNP-4C, however, TWODANT is used for neutron because it is difficult to precisely estimate the flux from the MA core to such small area as the window. TWODANT is suitable because it is determinstic.

The heat cross section is calculated by PHITS for whole energy region of proton and neutron. The DPA cross section for proton and neutron above 150 MeV is calculated by PHITS and that for neutron below 150 MeV is calculated by NJOY with LA150 as descrived in Ref. [4]. The production cross section of hydrogen and helium for proton and neutron above 20 MeV is calculated by PHITS and that for neutron below 20 MeV is obtained from a libraly of DCHAIN-SP, which is a calculation code for irradiation and decay. The library of DHCAIN-SP contains 150 groups cross sections for various reaction of neutron below 20 MeV such as (n,p), (n,np), (n,d), (n,α), and, etc. Those cross sections are collected from EFF-2.4, ADL-3.0, JEF-2.2, JENDL-3.2, etc.

4. Induced expressions for the damage

4.1. Parameters

Four parameters are chosen for parametric survey. Those are energy of proton beam (E_p), core criticality (k), material of the window (M) and beam shape (S) as shown

Table 2
Parameters for survey

Energy of the proton (GeV), E_p	0.6, 0.8, 1.0, 1.5[a] and 3.0
Core criticality, k	0.99, 0.97[a], 0.95 and 0.9
Material of the window, M	JPCA[a] and F82H
Shape of the proton beam, S	Gaussian[a] and Flat

[a] Reference values.

in Table 2. The parameters for the reference ADS are marked by asterisk. Compositions of the materials and the beam shape are shown in Table 3 and Fig. 3, respectively.

4.2. Beam current

At first, the core power is described by the next equation

$$P_c = \frac{C_t(E_p,k,S)N_p(E_p)}{\nu^{fiss}}\frac{\phi^*(E_p,k,S)}{\rho(k)}E^{fiss}, \quad (1)$$

where P_c (W) is the core power, $C_t(E_p,k,S)$ (A) is the beam current, $N_p(E_p)$ is the number of the spallation neutron, $\nu^{fiss}(=3.0)$ is the number of fission neutron by fission, $\phi^*(E_p,k,S)$ is spallation source effectiveness that is ratio of multiplication of spallation source to fission source in MA core, $\rho(k)$ is reactivity defined as $\rho(k)=1/k-1$ and $E^{fiss}(=202.6\times10^6)$ (eV) is a power generated by fission. Then the proton beam current is given by the Eq. (2).

$$C_t(E_p,k,S) = \frac{P_c\nu^{fiss}\rho(k)}{N_p(E_p)\phi^*(E_p,k,S)E^{fiss}}. \quad (2)$$

The current is depend on parameters, E_p, k and S, not on M.

$N_p(E_p)$ only depends on E_p as shown in Fig. 4, and is approximately expressed by linear function as

$$N_p(E_p) = 41.8\times(E_p-0.236). \quad (3)$$

The linear function for $N_p(E_p)$ is fitted neglecting the result for 3.0 GeV. The difference between the function and the result at 3.0 GeV is 9%. $\phi^*(E_p,k,S)$ depends on E_p, k and S as shown in Fig. 5, and its expressions are induced as

$$\phi^*(E_p,S,k) = \begin{cases}(1.582/N_p-0.527)\rho+(-1.840/N_p+0.771), & S=\text{Gauss}\\ (1.633/N_p-0.536)\rho+(-1.835/N_p+0.776), & S=\text{Flat}\end{cases}. \quad (4)$$

Difference between calculated result and Eq. (4) is smaller than 1%.

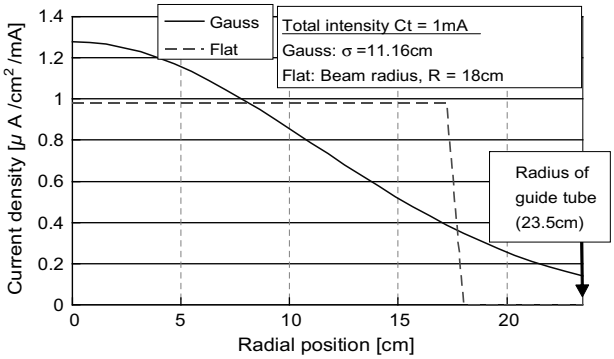

Fig. 3. Current density (beam shape).

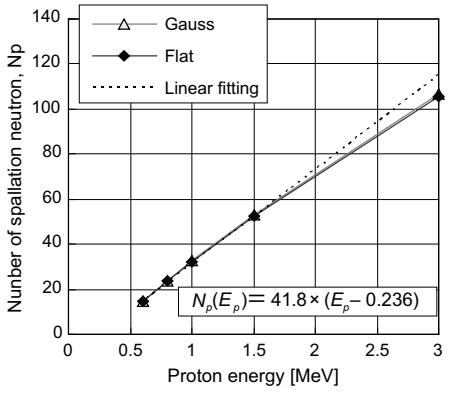

Fig. 4. Beam energy versus number of spallation neutron.

4.3. Flux

The reaction ratio in the window is obtained by

$$R^{reac}(E_p,k,M,S) = \sum_{par} X^{par,reac}(E_p,k,M,S)F^{par}(E_p,k,S), \quad (5)$$

where $R^{reac}(E_p,k,M,S)$ (/s) is a reaction rate, $X^{par,reac}(E_p,k,M,S)$ (cm^2) is a micro cross section and $F^{par}(E_p,k,S)$ (/cm^2/s) is a flux. 'par' means a kind of particle which is I (incident proton), P (proton without incident), N (high energy neutron above 10 MeV) and C (low energy neutron from the core below 10 MeV). 'reac' means kind of reaction, which is heat, DPA and production of ^{1}H, ^{2}H, ^{3}H, ^{3}He and ^{4}H.

Flux of incident proton, F^I, is proportional to the proton number passing the window as

Table 3
Chemical compositions of the window materials (wt%)

	Fe	Cr	Ni	Mo	Mn	Ti	Co	Cu	B
JPCA	65.27	14.14	15.87	2.34	1.54	0.22	0.028	–	0.004
F82H	89.62	7.87	0.02	0.003	0.1	0.004	–	0.01	–
	C	Si	P	S	N	V	Nb	W	Ta
JPCA	0.058	0.5	0.026	0.004	0.003	–	–	–	–
F82H	0.09	0.07	0.003	0.001	0.007	0.19	0.0002	1.98	0.03

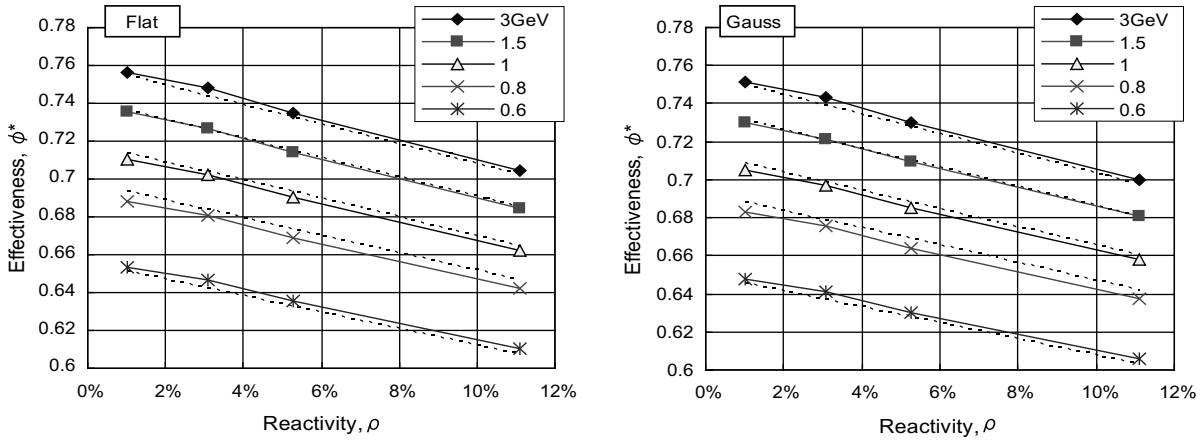

Fig. 5. Spallation source effectiveness, ϕ^* (E_p,k,S}).

$$F^{\mathrm{I}} = \frac{C_t}{e} \times \begin{cases} 12.6 \times 10^{-4}, & S = \text{Gauss} \\ 9.82 \times 10^{-4}, & S = \text{Flat} \end{cases}, \tag{6}$$

where e (C) is an electric constant. Flux of proton without incident, F^{P}, is expressed as the linear function of E_{P} as

$$F^{\mathrm{P}} = \frac{C_t}{e} \times \begin{cases} 3.95 \times 10^{-5} E_{\mathrm{p}} + 3.28 \times 10^{-5}, & S = \text{Gauss} \\ 2.62 \times 10^{-5} E_{\mathrm{p}} + 2.05 \times 10^{-5}, & S = \text{Flat} \end{cases} \tag{7}$$

As shown in Fig. 6, the difference between calculated result and Eq. (7) is 20% at the maximum, which is rather large. However, the reaction ratio of particle P is not dominant. Flux of high energy neutron, F^{N}, is not dependent on the beam shape as shown in Fig. 6, and expressed by the Eq. (8).

$$F^{\mathrm{N}} = \frac{C_t}{e} \times (9.79 \times 10^{-4} E_{\mathrm{p}} - 8.91 \times 10^{-5}),$$
$$S = \text{Gauss and Flat}. \tag{8}$$

As shown in Fig. 7, flux of low energy neutron below 10 MeV, F^{C}, depends on incident proton energy, E_{P}, and reactivity, ρ, but does not depend on the beam shape, S. F^{C} is expressed as

$$F^{\mathrm{C}} = \frac{C_t}{e} \times [(7.83 \times 10^{-4} E_{\mathrm{p}} - 1.81 \times 10^{-4})/\rho + (2.40 \times 10^{-2} E_{\mathrm{p}} + 3.89 \times 10^{-3})],$$
$$S = \text{Gauss and Flat}. \tag{9}$$

4.4. Cross section

As described in the previous section, the cross sections are mainly calculated by PHITS, and partly are given by the nuclear libraries. Figs. 8 and 9 show the cross section of heat and DPA for proton and neutron, respectively. The DPA cross section is same as Ref. [4].

The heat cross section is calculated by PHITS for whole energy region of proton and neutron with neglecting transportation of photon. The photon produced in the window is supposed to vanish without moving anywhere and generate heat there. Actually, the photons produced in the window and around the window outgo from or income to the window, and then generate heat. Heat generated in the win-

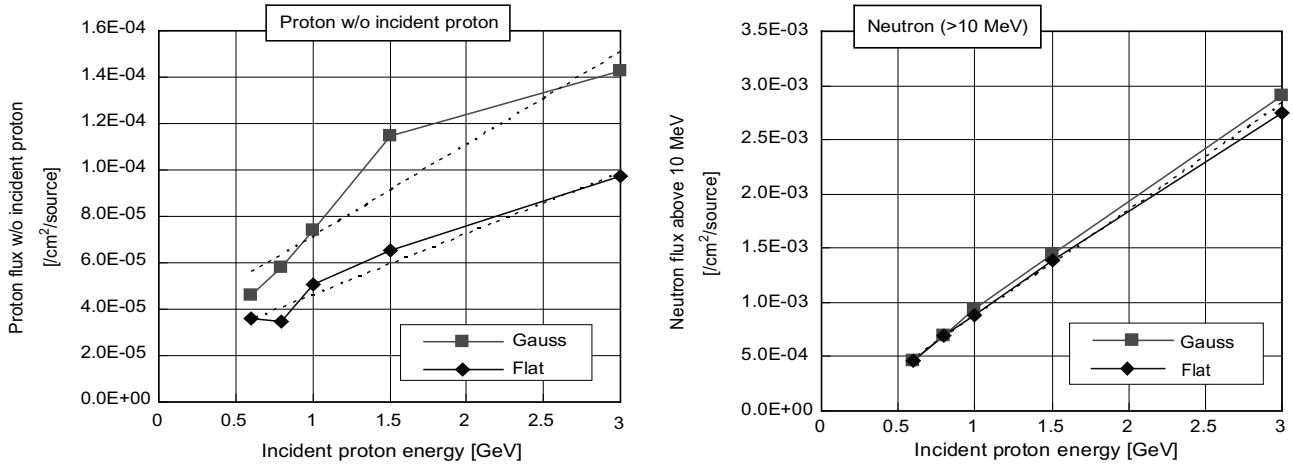

Fig. 6. Flux of proton without incident and high energy neutron above 10 MeV.

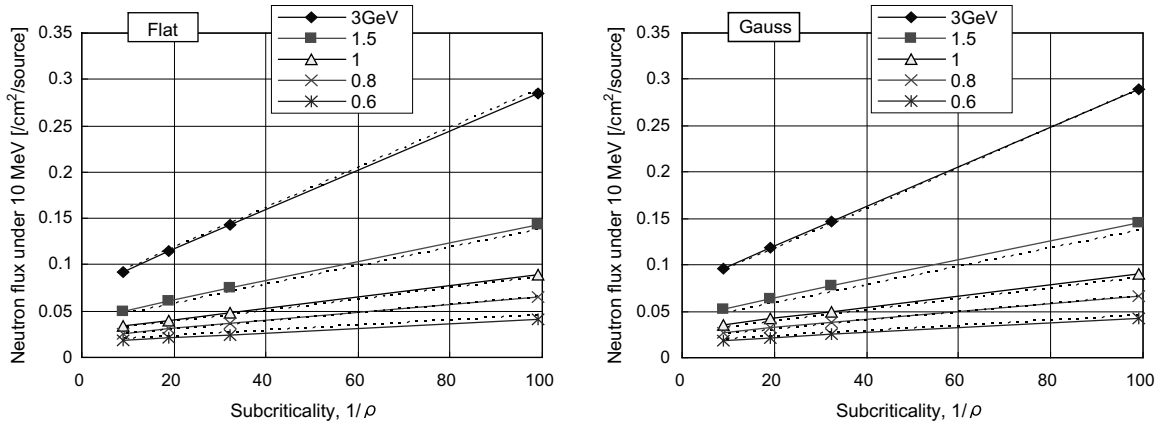

Fig. 7. Flux of low energy neutron below 10 MeV.

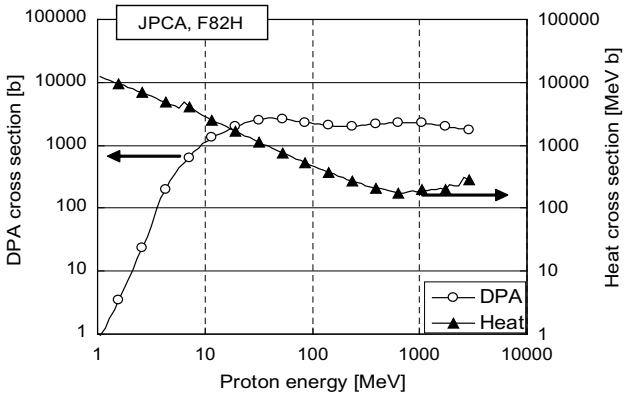

Fig. 8. DPA and heat cross section for proton.

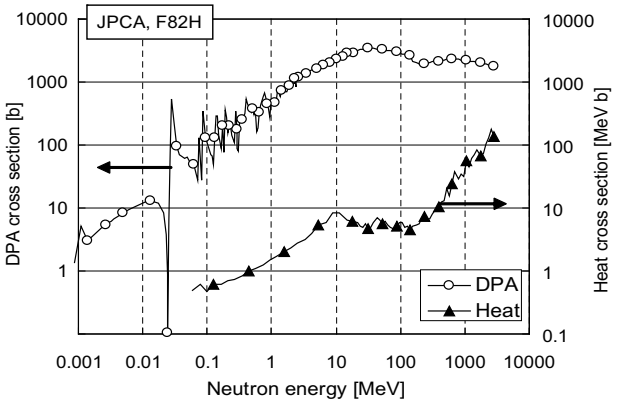

Fig. 9. DPA and heat cross section for neutron.

dow should be carefully calculated because the heat generated by photon is considerable. In the present calculation heat is overestimated because the present calculation is correct only when photon is produced uniformly around the window, while photon is produced only beside one-side of the window that is the target, and another side is the vacuum. The overestimation was 30% at the most. The overestimate tended to be large for high energy.

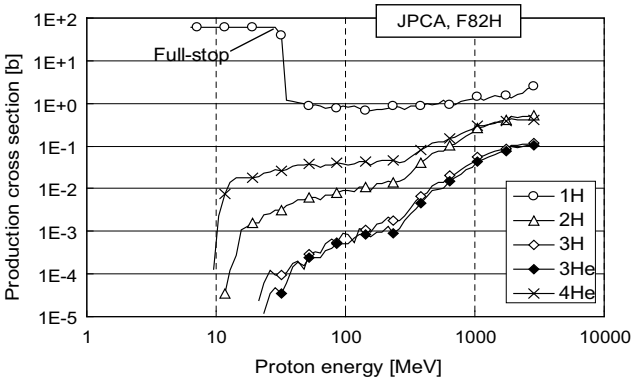

Fig. 10. Production cross section for proton.

Figs. 10–12 show the cross section of production by proton, neutron with JPCA and neutron with F82H, respectively. The cross section of ^{1}H production for the proton below 30 MeV is large because proton is fully stopped in the window with 2 mm in thickness. There are several gaps between PHITS calculation and nuclear library at 20 MeV of the neutron energy in Figs. 11 and 12. The gap of ^{1}H production is relatively large. This gap is important because the ^{1}H production by low energy neutron can not be neglected. The cross section of ^{1}H and ^{4}He produc-

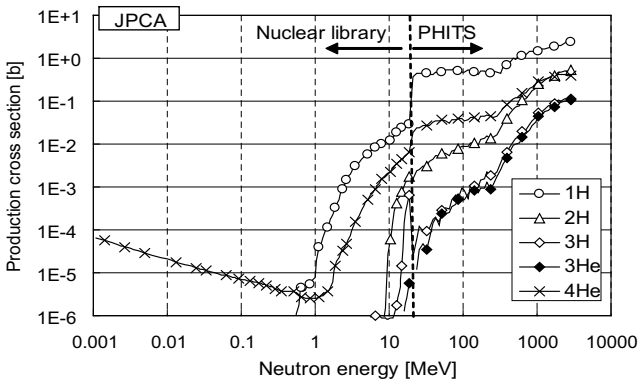

Fig. 11. Production cross section for neutron (JPCA).

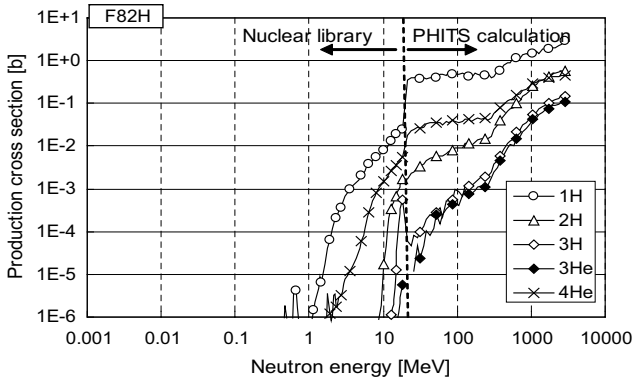

Fig. 12. Production cross section for neutron (F82H).

tion for the JPCA is slightly larger than that of F82H because of additions of nickel and boron. Based on these cross sections, one-group cross sections are calculated as following.

One-group cross sections for incident proton, $X^{\mathrm{I,reac}}$, are shown in Table 4. Because a reaction by incident protons is dominant, the approximate functions are not induced for accuracy. The cross section for proton without incident, $X^{\mathrm{P,reac}}$, and high energy neutron, $X^{\mathrm{N,reac}}$, is also shown in Table 4. They do not much depend on the incident energy, E_{P}, or are not dominant.

Before inducing expressions of the cross section for low energy neutron, $X^{\mathrm{C,reac}}$, averaged energy of neutron below 10 MeV, $E^{\mathrm{C}}_{\mathrm{Ave}}(E_{\mathrm{p}},k,S)$, is defined. $X^{\mathrm{C,reac}}$ is proportional to $E^{\mathrm{C}}_{\mathrm{Ave}}(E_{\mathrm{p}},k,S)$. $E^{\mathrm{C}}_{\mathrm{Ave}}(E_{\mathrm{p}},k,S)$ is in inverse proportion to incident energy, E_{P}, as shown in Fig. 13. There are several expressions of $E^{\mathrm{C}}_{\mathrm{Ave}}$ as shown in Fig. 13 because coefficients of linear functions are difficult to be expressed in the simple function of k .

As shown in Figs. 14–16, cross sections for low energy neutron are proportional to its averaged energy. Approximate functions induced are also shown in those figures. The production of ^{2}H, ^{3}H and ^{3}He by low energy neutron is omitted because they are too small.

5. Results and discussions

5.1. The reference ADS

Based on the expressions previously described, heat, DPA and nuclide productions are evaluated for the reference ADS with 0.97 of k, 1.5 GeV of the beam energy, JPCA window material and Gaussian beam shape. Table 5 shows flux, cross sections and result after 300 FPDs for each kind of particle. The heat density generated in the window was 375 W/cm^3, which is of course smaller than the limit of the present design, 700 W/cm^3.

Table 4
One-group cross sections of proton and high energy neutron

ParticleE_{p} (GeV)	I					P	N
	3	1.5	1	0.8	0.6	All	All
Heat (MeV b)	329	224	197	194	196	1010[a]	6.4[a]
DPA (b)	1861	2155	2269	2243	2279	2148[a]	1697[a]
^{1}H (b)	2.23	1.64	1.37	1.23	1.02	12.78[a]	0.338[a]
^{2}H (b)	0.67	0.37	0.24	0.18	0.12	0.013[b]	3.3E-3[a]
^{3}H (b)	0.15	0.083	0.050	0.036	0.023	1.9E-3[b]	3.4E-4[b]
^{3}He (b)	0.13	0.066	0.038	0.027	0.017	1.4E-3[b]	1.3E-4[b]
^{4}He (b)	0.50	0.36	0.28	0.23	0.18	0.039[a]	0.021[a]

[a] It does not depend on E_{P}.
[b] It depends on E_{P}, but a value is very small.

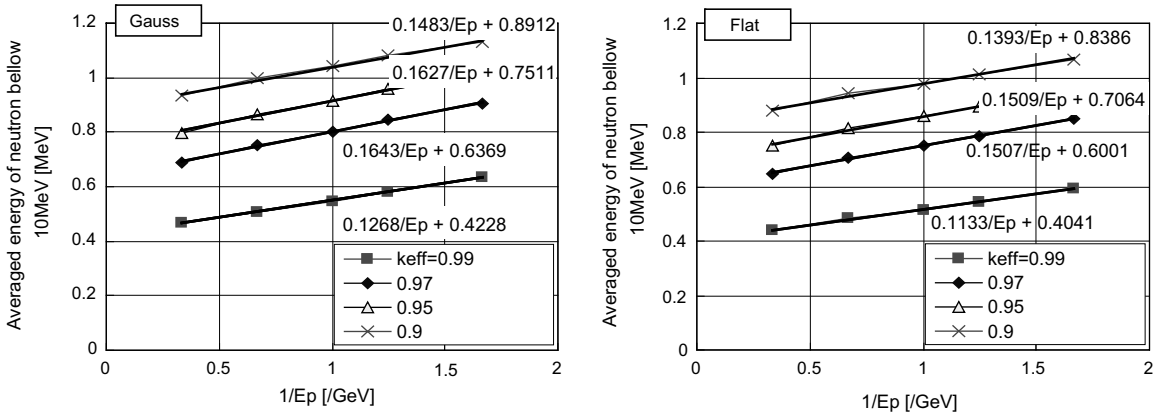

Fig. 13. Averaged energy of low energy neutron.

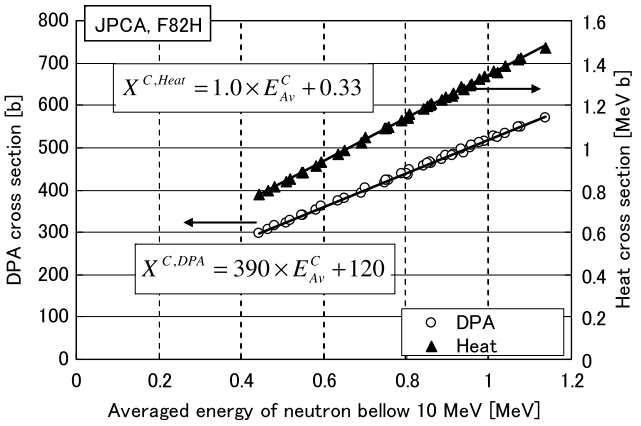

Fig. 14. One-group cross sections of DPA and heat for neutron.

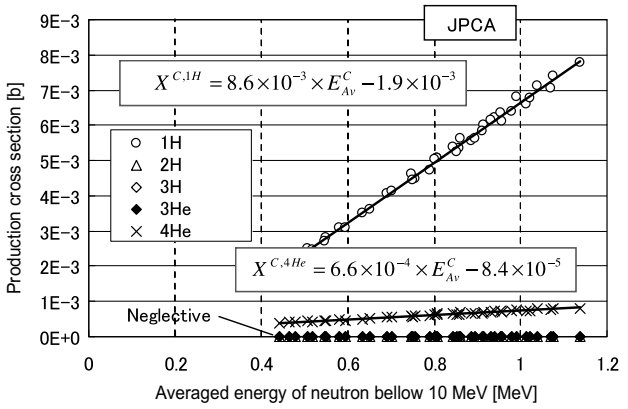

Fig. 15. One-group cross section of production for neutron (JPCA).

Displacement is dominated by the low energy neutron while all other reactions aside from the displacement reactions are dominated by the incident proton. The production of ^{2}H, ^{3}H and ^{3}He by the low energy neutron is very small, but that of ^{1}H and ^{4}He cannot be neglected.

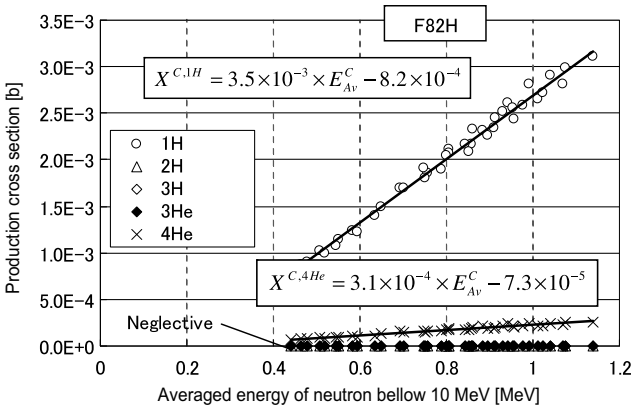

Fig. 16. One-group cross section of production for neutron (F82H).

5.2. Effect of criticality swing

As shown in Fig. 2, the beam current of the reference ADS changes between 9.6 and 21 mA following the criticality swing. The beam window is maximally damaged during 900–1200 FPDs. The proton beam current averaged during this term is 19.2 mA, which is twice the initial current, 9.6 mA. It is important to reduce criticality and current swing to reduce heat, DPA and gas productions because they are almost proportional to the current as shown in Table 6.

5.3. Survey of beam energy

Fig. 17 shows the result of parameters survey for the beam energy. The more the proton beam energy is, the less the window is damaged. Because the design for the window with the heat density more than 700 W/cm^3 is difficult, the proton beam energy above 1.0 GeV is preferable. Heat, DPA and gas productions tend to be insensitive to the proton beam energy above 1.5 GeV. Considering the technical

Table 5
Damage on the window in the reference ADS after 300 FPDs

Particle		*I*	*P*	*N*	*C*	Total
Flux (/cm^2/s)		7.57*E* + 13	5.53*E* + 12	8.28*E* + 13	4.32*E* + 15	4.49*E* + 15
Averaged energy (MeV)		1500	107	42	0.75	
Cross section (b)	Heat (MeV b)	224	1010	6.4	1.1	
	DPA	2155	2148	1697	419	
	^{1}H	1.59	12.78	0.338	4.5E-3	
	^{2}H	0.37	0.013	3.3E-3	7.3E-7	
	^{3}H	0.083	1.9E-3	3.4E-4	4.9E-7	
	^{3}He	0.066	1.4E-3	1.3E-4	3.5E-11	
	^{4}He	0.36	0.039	0.021	5.8E-4	
Reaction	Heat (W/cm^3)	229	75	7.2	63	375
	DPA (300 FPDs)	4.2	0.31	3.6	47	55
	^{1}H (appm,300 FPDs)	3119	1831	725	503	6179
	^{2}H (appm,300 FPDs)	727	1.8	7.2	0.082	736
	^{3}H (appm,300 FPDs)	163	0.27	0.72	0.054	164
	^{3}He (appm,300 FPDs)	130	0.20	0.28	3.9E-6	130
	^{4}He (appm,300 FPDs)	709	5.5	45	65	825

Table 6
Heat, damage and gas production during 900–1200 FPDs

	Initial	900–1200 FPDs
Current (mA)	9.6	19.2
Maximum heat (W/ cm^3)	375	802
DPA (300 FPDs)	55	98
^{1}H (appm,300 FPDs)	6179	12295
^{2}H (appm,300 FPDs)	736	1466
^{3}H (appm,300 FPDs)	164	327
^{3}He (appm,300 FPDs)	130	260
^{4}He (appm,300 FPDs)	825	1631

issues on performance of the accelerator, it is appropriate in the viewpoint of the window damage to adopt 1.5 GeV of E_p as the reference.

5.4. Survey of criticality

Fig. 18 shows the result of survey for the criticality. Heat, DPA and gas productions are linearly decrease by depending on criticality, k. The value of k close to 1.0 is clearly superior. On the contrary, k below 0.95 is difficult

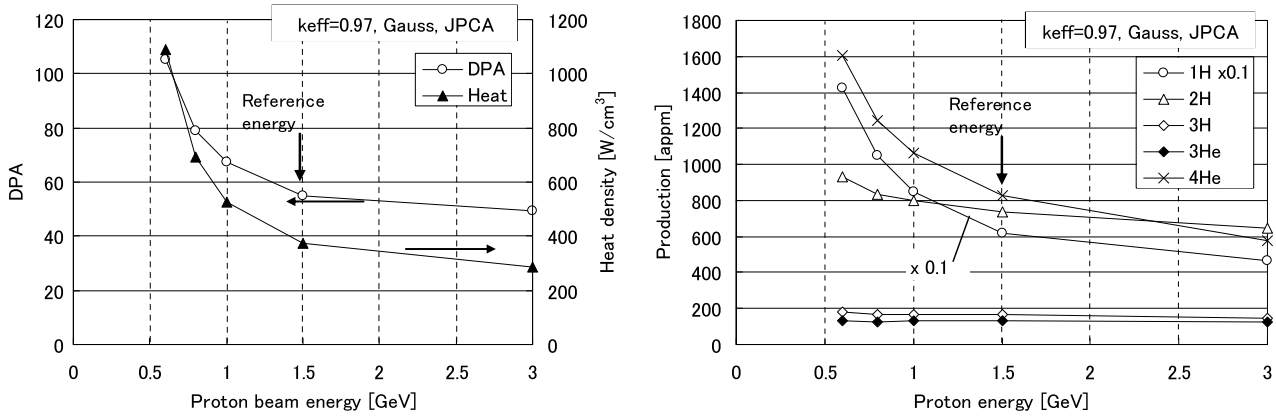

Fig. 17. Survey for proton beam energy, E_p.

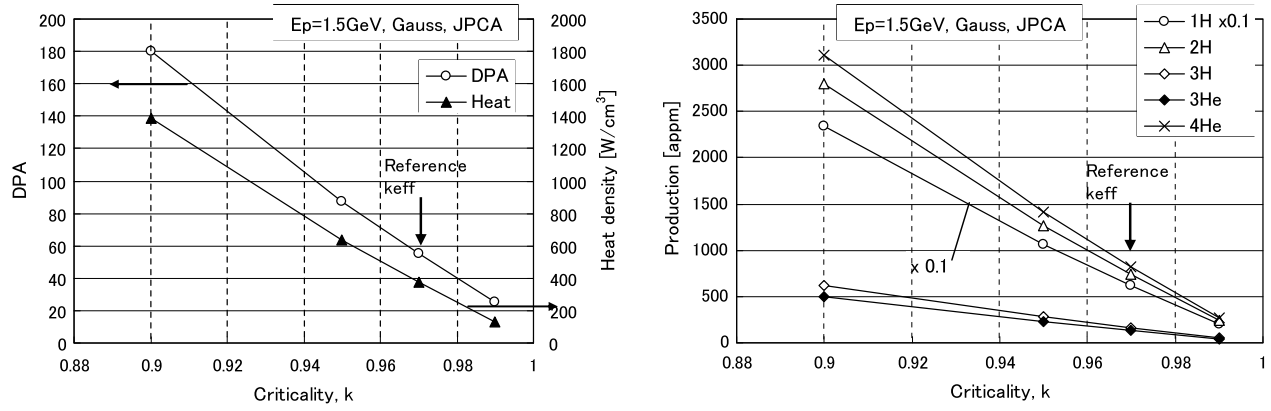

Fig. 18. Survey for criticality, k.

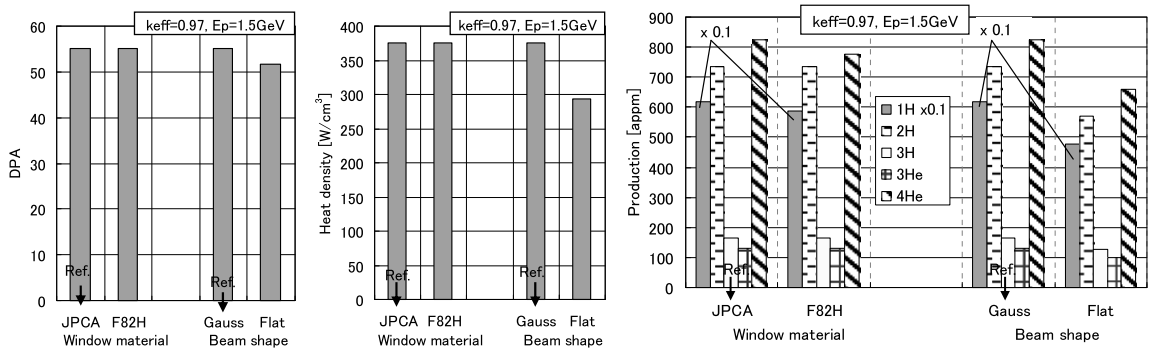

Fig. 19. Survey for the window, material and beam shape.

because the heat density is beyond 700 W/cm^3. However, k is limited below 0.97 by critical safety issues such as temperature reactivity, system cool-down reactivity and uncertainties as described in Ref. [1]. Therefore, the reference value of k is 0.97 in the present ADS, but it is possible to be closer to the critical to reduce heat, DPA and gas productions on the window if they avoid the feasibility of the ADS.

5.5. Survey of material and beam shape

Fig. 19 shows the result of survey for the window material and beam shape. Heat and displacement do not depend on the kind of material. The production of ^{1}H in the case of JPCA is slightly larger than F82H because of the addition of nickel, which reacts with low energy neutron and releases proton. The production of ^{4}He is also larger because of the addition of boron to JPCA, even though the addition of 0.004 wt% is quite small.

The Gaussian beam shape is inferior to the flat beam because the current density at the center of the window is larger than flat beam. Flattening of beam shape is desirable.

6. Conclusion

Heat, displacement and production of hydrogen and helium were evaluated for the ADS with several parameters. The flux of proton and neutron was calculated by PHITS and TWODANT. The cross sections were calculated by PHTIS without displacement by neutron below 150 MeV and production by neutron below 20 MeV.

Approximate expressions for the proton beam current, the number of spallation neutrons and spallation source effectiveness were induced as functions of four parameters; those are, proton beam energy, criticality, window material, and beam shape. The expressions for the flux and cross sections were also induced. Then heat, DPA and gas productions are possibly evaluated without numerical calculation. As the result of estimation for the reference ADS, heat and gas productions were dominated by the incident proton. DPA was dominated by the low energy neutron from the MA core. Heat and gas production of ^{1}H and ^{4}He by the low energy neutron could not be neglected. Heat, DPA and gas production were twice the reference values during the most severe operation term of the reference ADS. It is important to reduce criticality and current swing.

As the result of survey for the beam energy, the more the proton beam energy was, the less the window was damaged. Because heat, DPA and gas productions tended to be insensitive to the proton beam above 1.5 GeV of E_p, it is appropriate to adopt 1.5 GeV of E_p as the reference. As the result of survey of for criticality, criticality close to the critical was clearly superior. The trade-off between the damage and criticality safety should be considered. As the result of other surveys, the gas production of ^{1}H and ^{4}He in JPCA was slightly larger than that of F82H because of the addition of nickel and boron. Flattening of beam shape was desirable to reduce heat, DPA and gas productions.

Further study for a life time estimation in the ADS environment is necessary based on the irradiation damage presented in the present report, hydraulic analysis, stress analyses and irradiation tests.

References

[1] K. Tsujimoto et al., J. Nucl. Sci. Technol. 41 (1) (2004) 21.
[2] H. Iwasa, K. Niita, T. Nakamura, J. Nucl. Sci. Technol. 39 (2002) 1142.
[3] R.E. Alcouffe et al., LA-10049-M, 1990.
[4] M. Harada et al., J. Nucl. Mater. 343 (2005) 197.
[5] T. Kai et al., JAERI-Data/Code 2001-016, 2001 (in Japanese).
[6] H. Oigawa et al., in: Workshop Proceedings of Utilization and Reliability of High Power Proton Accelerators, OECD/NEA, 2005, p. 325.